Heliyon 9 (2023) e20011

Contents lists available at ScienceDirect

Heliyon

journal homepage: www.cell.com/heliyon

Development and evaluation of a novel chromium III-based compound for potential inhibition of emerging SARS-CoV-2 variants

Yu-Jung Lin [a,b], Navaneethan Sundhar [a,c], Hema Sri Devi [a], Hsueh-Fa Pien [d], Shina Fong-Mei Wen [d], Jenn-Line Sheu [d], Bruce Chi-Kang Tsai [a], Chih-Yang Huang [a,c,e,f,g,*]

[a] *Cardiovascular and Mitochondrial Related Disease Research Center, Hualien Tzu Chi Hospital, Buddhist Tzu Chi Medical Foundation, Hualien, Taiwan*
[b] *School of Post-Baccalaureate Chinese Medicine, College of Medicine, Tzu Chi University, Hualien, Taiwan*
[c] *Graduate Institute of Biomedical Sciences, School of Medicine, China Medical University, Taichung, Taiwan*
[d] *TOMA Biotechnology CO., LTD, Taipei, Taiwan*
[e] *Department of Medical Research, China Medical University Hospital, Taichung, Taiwan*
[f] *Center of General Education, Buddhist Tzu Chi Medical Foundation, Tzu Chi University of Science and Technology, Hualien, Taiwan*
[g] *Department of Medical Laboratory Science and Biotechnology, Asia University, Taichung, Taiwan*

ARTICLE INFO

Keywords:
COVID-19
ACE2
TMPRSS2
Chromium (III)-Based compound
SARS-CoV-2

ABSTRACT

Severe acute respiratory syndrome coronavirus 2 (SARS-CoV-2) has caused 403 million cases of coronavirus disease (COVID-19) and resulted in more than 5.7 million deaths worldwide. Extensive research has identified several potential drug treatments for COVID-19. However, the development of new compounds or therapies is necessary to prevent the emergence of drug resistance in SARS-CoV-2. In this study, a novel compound based on hexaacetotetraaquadihydroxochromium(III) diiron(III) nitrate, which contains small amounts of chromium (III), was synthesised and evaluated for its effectiveness against multiple variants of COVID-19 using both *in vitro* and *in vivo* models. This innovative compound demonstrated interference with the interaction between the spike protein of SARS-CoV-2 and angiotensin-converting enzyme 2 (ACE2). Furthermore, *in vitro* experiments showed that this compound downregulated the expression of ACE2 and transmembrane serine protease 2 (TMPRSS2). It also exhibited a reduction in the activity of 3-chymotrypsin-like protease (3CL) and RNA-dependent RNA polymerase (RdRp). Pretreatment with this small chromium (III)-based compound resulted in reduced ACE2-rich cell infection by various variants of SARS-CoV-2 spike protein-pseudotyped lentivirus. Finally, the compound effectively inhibited viral infection by multiple variants of SARS-CoV-2 spike protein-pseudotyped lentivirus in both the abdominal and thoracic regions of mice. In conclusion, this compound lowers the likelihood of SARS-CoV-2 entry into cells, inhibits viral maturation and replication *in vitro*, and reduces infection levels of multiple variants of SARS-CoV-2 spike protein-pseudotyped lentivirus in the abdomen and thorax following pretreatment. Small chromium (III)-based compounds have the potential to restrict the progression of SARS-CoV-2 infections.

* Corresponding author. Cardiovascular and Mitochondrial Related Disease Research Center, Hualien Tzu Chi Hospital, Buddhist Tzu Chi Medical Foundation, Tzu Chi University of Science and Technology, Hualien, Taiwan.
E-mail address: cyhuang@mail.cmu.edu.tw (C.-Y. Huang).

https://doi.org/10.1016/j.heliyon.2023.e20011
Received 25 January 2023; Received in revised form 18 August 2023; Accepted 8 September 2023
Available online 9 September 2023

1. Introduction

Severe acute respiratory syndrome coronavirus 2 (SARS-CoV-2) is an enveloped single-stranded positive-sense RNA virus with a genome of approximately 30,000 nucleotides [1]. It first emerged in Wuhan, Hubei Province, People's Republic of China, causing the novel coronavirus disease 2019 (COVID-19). From the end of 2019 to early 2020, COVID-19 rapidly spread worldwide and was declared a pandemic [2]. As of February 2022, the World Health Organisation (WHO) has reported 403 million COVID-19 cases and more than 5.7 million deaths across 220 countries (source: https://covid19.who.int). This novel coronavirus shares similarities with the SARS-CoV responsible for the 2002 SARS pandemic, but SARS-CoV-2 exhibits higher infectiousness, resulting in a pandemic [3]. The genome of SARS-CoV-2 is 80% similar to that of SARS-CoV and approximately 96% identical to the bat coronavirus BatCoV RaTG13 [4]. The emergence of viral variants has impacted the development and efficacy of vaccines [5]. Despite some effective therapies identified for COVID-19, there is an urgent need to develop universal vaccines and effective drugs to combat this pandemic. Additionally, existing vaccines have shown reduced efficacy over time due to the emergence of SARS-CoV-2 variants such as the alpha, delta, and omicron variants, with the latter being the current primary concern [6,7].

SARS-CoV-2 generally comprises proteins with structural functions (envelope, nucleocapsid, membrane, and spike) as well as nonstructural functions (NSP1 to NSP10 and NSP12 to NSP16) [8]. Entry of SARS-CoV-2 into host cells requires angiotensin-converting enzyme 2 (ACE2) as a receptor and transmembrane serine protease 2 (TMPRSS2) on the host cell surface to facilitate cell entry [9]. The viral spike proteins bind to host ACE2 receptors and are cleaved by TMPRSS2, leading to fusion between the viral and host membranes. Consequently, inhibiting the expression and function of ACE2 and/or TMPRSS2 could be a potential strategy to prevent SARS-CoV-2 entry into host cells [10]. After entering host cells, SARS-CoV-2 releases its viral RNA genome, and the unstructured amino acid sequences, polyproteins 1a and 1 ab, are translated in the cytoplasm. These polyproteins are cleaved by papain-like and 3C-like proteases to form 16 nonstructural proteins that serve as replication-transcription complexes. Structural proteins, encoded at the 3′ ends, play essential roles in virus maturation and transmission [4]. Transcription-replication complex proteins, including RNA-dependent RNA polymerase (RdRp), facilitate viral RNA replication. Viral structural proteins translated from viral RNA are inserted into the endoplasmic reticulum, and viral genome packaging occurs at the endoplasmic reticulum-Golgi interface. Finally, mature SARS-CoV-2 is released from host cells via the constitutive exocytic pathway [11,12]. Several drugs, including lopinavir, molnupiravir, nirmatrelvir, remdesivir, and ritonavir, have shown potential as treatment options for COVID-19 [13–16], with some being used to reduce COVID-19 severity in clinical settings. While some SARS-CoV-2-infected individuals remain asymptomatic, others experience cold or flu-like symptoms and may develop severe complications such as hypoxia and pneumonia, which can be fatal [17]. Even after recovery, COVID-19 can have long-term health consequences [18]. Therefore, the development of medications and therapies to prevent and treat SARS-CoV-2 infection is crucial. New treatments are necessary to combat the emergence of drug-resistant viruses.

Previous studies have investigated the use of various drugs, including lopinavir, molnupiravir, nirmatrelvir, remdesivir, and ritonavir, for COVID-19 treatment [13–16]. Some of these drugs have been employed to reduce the severity of COVID-19 in clinical settings. However, the emergence of viral drug resistance necessitates the development of novel compounds or therapies. In this study, we synthesised a novel chromium (III)-based compound, hexaacetotetraaquadihydroxochromium(III)diiron(III) nitrate $[CrFe_2(CH_3CO_2)_6(H_2O)_4(OH)_2]^{+}NO_3^{-}$ (Fig. 1), and investigated its effects on multiple SARS-CoV-2 variants using cell and animal models.

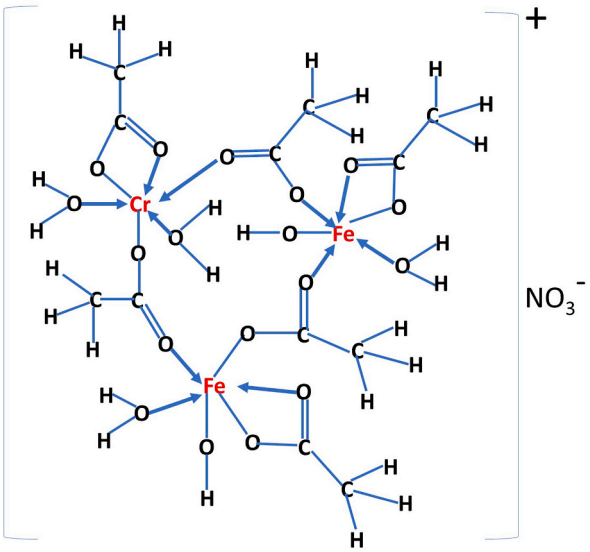

Fig. 1. Structure of a novel small chromium (III)-based compound.

2. Materials and methods

2.1. Materials

All chemicals utilised in this study were of analytical grade and procured from Sigma-Aldrich (St. Louis, MO, USA) and Merck (Darmstadt, Germany), unless specified otherwise. Hexaacetotetraaquadihydroxochromium(III)diiron(III) nitrate was synthesised by TOMA BIO. Co. Ltd., (Taipei, Taiwan) and dissolved in Phosphate Buffered Saline (PBS). Primary antibodies against ACE2 (sc-390851) and β-actin (sc-47778) were obtained from Santa Cruz Biotechnology (Santa Cruz, CA, USA), while TMPRSS2 (ab92323) was acquired from Abcam (Cambridge, UK). Various fluorescent SARS-CoV-2 spike pseudotyped lentiviral particles representing different variants were procured from RNAicore (Academia Sinica, Taipei, Taiwan). The preparation of viral particles was performed following established protocols [19,20].

2.2. SARS-CoV-2 spike protein-ACE2 binding assay

The COVID-19 Spike-ACE2 Binding Assay Kit from RayBiotech (Peachtree Corners, GA, USA) was utilised to assess the impact of the chromium (III)-based compound on the binding affinity between ACE2 receptors and the SARS-CoV-2 spike protein, following the manufacturer's protocol. An optically clear flat-bottom 96-well plate was employed for the *in vitro* enzyme-linked immunosorbent assay. Various concentrations of the chromium (III)-based compound were added to the ACE2 protein mixture and incubated in 96-well plates containing recombinant SARS-CoV-2 Spike binding domain protein that had been pre-coated, while shaking at 200 rpm at 22 °C for 2.5 h. Subsequently, the plate was washed four times using 300 μL of wash buffer, and the primary antibody (goat anti-ACE2 antibody) was added to each well. This washing step was repeated three times. Next, horseradish peroxidase-conjugated anti-goat secondary antibody was added to each well, and the entire plate was incubated with shaking at 200 rpm at 22 °C for 60 min. Following this, 100 μL of 3,3′,5,5′-tetramethylbenzidine one-step substrate was added to each well, and the plate was once again incubated in a dark location, while shaking at 200 rpm at 22 °C for 60 min. The reaction was terminated by adding a 50 μL stop solution, and the absorbance of each well was measured at 405 nm using a multimode plate reader.

2.3. Cell culture

Calu-3 human lung adenocarcinoma cell lines (ATCC HTB-55 and P8–P10) and Caco-2 human colorectal adenocarcinoma cell lines (ATCC HTB-37 and P8–P10) were obtained from the American Type Culture Collection (ATCC, Manassas, VA, USA). Both cell lines were maintained in Eagle's Minimum Essential Medium supplemented with 20% foetal bovine serum (Gibco™, Thermo Fisher Scientific, Waltham, MA, USA) and 1% penicillin/streptomycin. Human bronchial epithelial cells BEAS-2B (95102433, Sigma-Aldrich) were cultured in low glucose DMEM medium (Gibco, USA) with 10% foetal bovine serum and 1% penicillin/streptomycin. The cells were cultured at 37 °C in a humidified incubator with 95% air and 5% CO_2.

2.4. Cell viability assay

BEAS-2B cells were seeded in triplicate into 96-well plates, and various concentrations of chromium (III)-based compounds were administered. Following a 24-h treatment period, the cells were exposed to 0.5 mg/mL of MTT [3-(4,5-dimethylthiazol-2-yl)-2,5-diphenyltetrazolium-bromide] reagent and incubated in a humidified atmosphere with 5% CO2 at 37 °C for 2 h. After incubation, the formazan crystals were dissolved in dimethyl sulfoxide (DMSO), and the absorbance was measured at 570 nm using an ELISA reader. Three independent experiments were conducted, following the previously described protocol. Cell viability was calculated as a percentage of the control using the following formula: (treated − blank)/(untreated control − blank) × 100%.

2.5. Western blot

For Western blot analysis, the cultured cells were rinsed twice with PBS and harvested using a scraper. The collected cells were then centrifuged at 3000 rpm for 10 min to remove the PBS. Subsequently, the cell pellet was treated with RIPA buffer containing protease and phosphatase inhibitors and gently vortexed to homogenise the samples. The samples were incubated on ice for 1 h and then centrifuged at 12,500 rpm for 30 min at 4 °C. The resulting supernatant was collected, and the protein concentration was determined. To prepare the protein samples, sterile water and 5 × loading dye were added and the mixture was boiled at 95 °C for 10 min. The protein samples were separated using 10% sodium dodecyl sulphate-polyacrylamide gel electrophoresis (SDS-PAGE) at 100 V. After separation, the protein samples were transferred to a 0.2 μm PVDF membrane (88520, Thermo Fisher Scientific) at 60 V for 120 min. The membranes were then blocked with 5% skim milk buffer at 25 °C for 60 min. Subsequently, the blocked membranes were incubated with primary antibodies at 4 °C for more than 12 h. On the following day, the membranes were washed and incubated with secondary antibodies at 25 °C for 1 h on a shaker. The blots were visualised using a chemiluminescent reagent (WesternBright® ECL) and captured using an iBright 1500 luminescent image analyser, as previously described [21–23].

2.6. Quantification of 3-chymotrypsin-like protease (3CL) activity

The SensoLyte® 520 SARS-CoV-2 3CL Protease Activity Assay Kit (AS-72262, Kaneka Eurogentec S.A., Seraing, Belgium) was utilised to assess the impact on fluorescence resulting from the cleavage of the FRET peptide substrate by the 3CL protease. The experimental procedure provided by the manufacturer was strictly followed. Aliquots of 40 μL of enzyme solution were combined with 10 μL of the chromium (III)-based compound in a 96-well plate. Separate wells were designated for positive, vehicle, inhibitor, test compound, and substrate controls. A total volume of 50 μL of the reaction mixture was added to each well and incubated for 30 min. The protease activity was then measured at 490 nm/520 nm using a multimode plate reader.

2.7. The activity assay of RNA-dependent RNA polymerase (RdRp)

We employed a Viral (Flavivirus) RNA-dependent RNA polymerase assay kit (ProFoldin, Hudson, MA, USA) to evaluate the impact of chromium (III)-based compounds on RdRp activity. The manufacturer's protocol was strictly adhered to throughout the experiment. A reaction mixture of 30 μL was prepared and incubated at 37 °C for 60 min. Following incubation, a 1x fluorescence dye was added to the reaction mixture, and the fluorescence intensity was measured at 535 nm using a multimode plate reader.

2.8. Assay of SARS-CoV-2 spike protein pseudotyped lentivirus in ACE2 rich bronchial cells (Calu-3) and colorectal cells (Caco-2)

A total of 2×10^3 cells were seeded onto a chamber slide and incubated overnight. Subsequently, the cells were pretreated with a chromium (III)-based compound. After 12 h, fluorescent SARS-CoV-2 spike protein pseudotyped lentiviruses were introduced, and the cells were incubated for 48 h. Following this, the cells were washed with PBST and sealed with mounting medium. All images were captured using an Axio Observer 207 A1 digital fluorescence microscope (Olympus, Tokyo, Japan).

2.9. The design of SKH1 mice experiments

All experiments were conducted in accordance with the protocols approved by the Institutional Animal Care and Ethics Committee (IACUC) of Hualien Tzu Chi Hospital, Hualien, Taiwan (approval number 109–50). The SKH1 mice provided by Dr. Tzu-Kai Lin were housed in a controlled environment with a 12/12-h light/dark cycle, at a temperature of 24 ± 2 °C and humidity maintained at 55 ± 10%. They were provided with a standard laboratory diet (PMI Nutrition International, Brentwood, MO, United States) and access to reverse osmosis-treated water. For evaluating the impact of the chromium (III)-based compound on viral adhesion and the infective viral load of multiple variants of SARS-CoV-2, eight-week-old SKH1 mice were utilised. The treated mice received oral pretreatment of 200 μL of the chromium (III)-based compound at doses of either 10 mg/mouse/day or 100 mg/mouse/day for three consecutive days. The control group mice were administered the vehicle, PBS. Starting from the fourth day, in addition to the chromium (III)-based compound administration, the mice were intranasally infected with 500 μL of 1.2×10^6 pseudotyped lentiviral particles daily for three consecutive days, using a nebuliser (Aeroneb USB controller, Kent Scientific Corporation Torrington, CT, USA) at a flow rate of 0.4 mL/min. On the seventh day, the pseudotyped lentiviral particle load accumulation in the mice was determined using an *In Vivo* Imaging System (IVIS, PerkinElmer, UK). Each group consisted of nine mice.

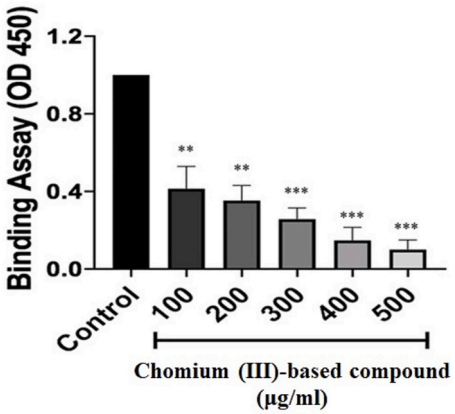

Fig. 2. Effect of the chromium (III)-based compound on the interaction between rhACE2 and the SARS-CoV-2 Spike (RBD) protein. The interaction between the spike (RBD) glycoprotein and rhACE2 was measured using the SARS-CoV-2 Spike-ACE2 binding assay with different doses (up to 500 μg) of the chromium (III)-based compound. $^{**}p < 0.01$; $^{***}p < 0.001$.

2.10. Statistical analysis

Statistical comparisons were conducted using GraphPad Prism software (version 7.0; GraphPad Software, San Diego, CA, USA). Differences between groups were statistically analysed utilising one-way analysis of variance, followed by Tukey's multiple comparison tests. Data are presented as means ± standard deviation. A significance level of $p < 0.05$ was considered statistically significant [24,25].

3. Results

3.1. Novel small chromium (III)-based compound disrupts the interaction between the SARS-CoV-2 spike protein and ACE2

In order to assess the ability of the novel small chromium (III)-based compound to inhibit the interaction between SARS-CoV-2 spike proteins and ACE2 in host cells, we utilised SARS-CoV-2 Spike-ACE2 binding assay kits for confirmation. The results

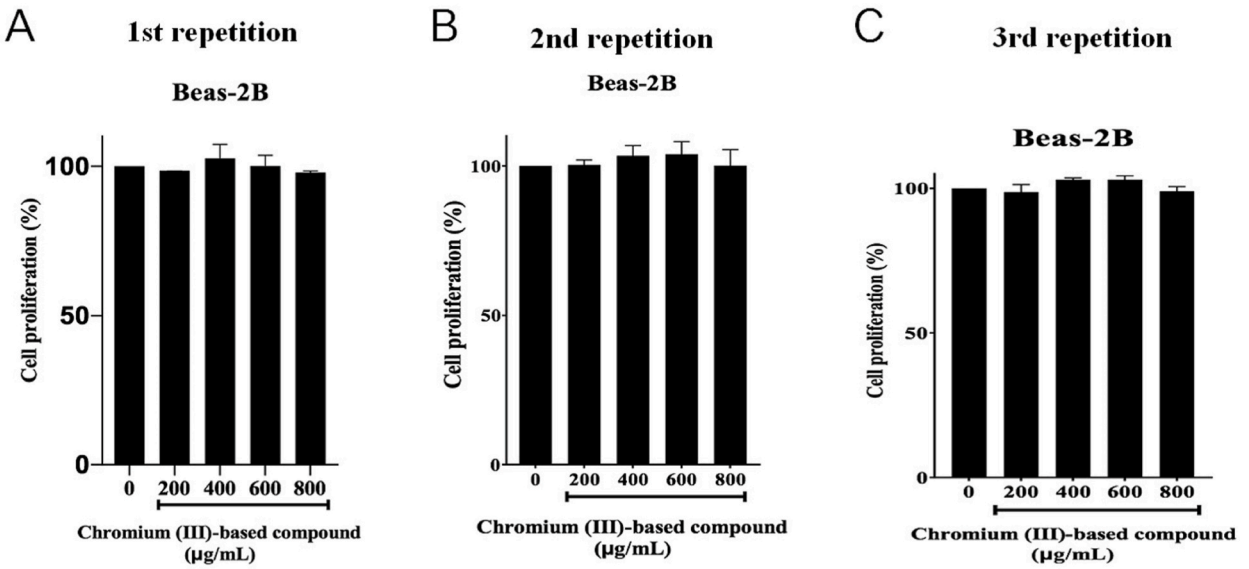

Fig. 3. Effect of the chromium (III)-based compound on cytotoxicity. The potential of the chromium (III)-based compound to induce cytotoxicity was investigated using BEAS-2B cells and the MTT assay. Doses ranging from 200 to 800 μg/mL of the chromium (III)-based compound did not significantly inhibit cell survival rate in BEAS-2B cells. (A) First biological repeat. (B) Second biological repeat. (C) Third biological repeat.

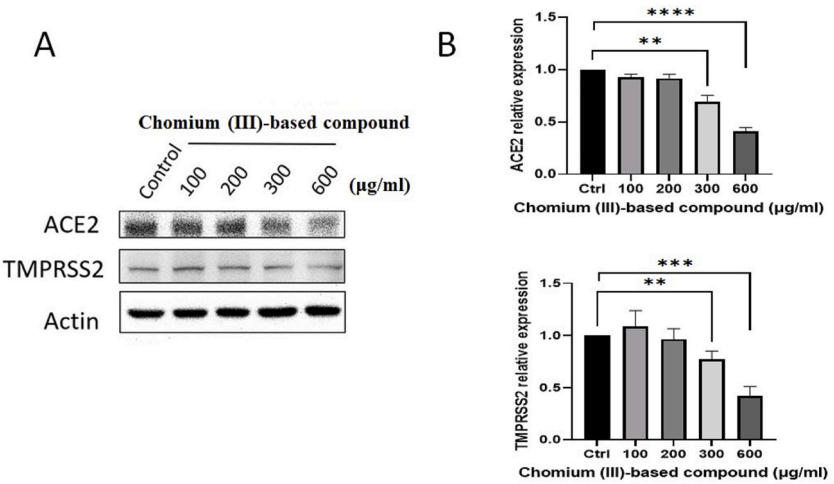

Fig. 4. Effect of the chromium (III)-based compound on the expression of ACE2 and TMPRSS2. (A) Western blotting was used to determine the dose-dependent changes in the expression of ACE2 and TMPRSS2 proteins in response to the chromium (III)-based compound at doses of 300 and 600 μg. (B) Dose-dependent effects of chromium(III)-based compounds on target signalling molecules relative to untreated control cells.

indicated that the small chromium (III)-based compound exhibited a dose-dependent inhibition of the binding between the viral SARS-CoV-2 spike protein and ACE2 (Fig. 2), highlighting its potential to inhibit the interaction between the SARS-CoV-2 spike protein and ACE2 in host cells.

3.2. Effect of the chromium (III)-based compound on ACE2 and TMPRSS2 expression

Subsequently, we employed BEAS-2B cells and the MTT assay to investigate the potential cytotoxicity induced by chromium (III)-based compounds. As anticipated, doses ranging from 200 to 800 μg/mL of the chromium (III)-based compound did not significantly inhibit cell survival rate in BEAS-2B cells (Fig. 3). These findings demonstrate that chromium (III)-based compounds do not exert cytotoxic effects on cell growth. Additionally, we assessed the impact of the chromium (III)-based compound on the protein expression of ACE2 and TMPRSS2, which are crucial for viral infectivity and facilitate viral cell membrane fusion. The results indicated a dose-dependent inhibition of ACE2 and TMPRSS2 protein expression in Calu-3 cells after 24 h with doses of 300–600 μg/mL of the chromium (III)-based compound (Fig. 4). Given the critical roles played by ACE2 and TMPRSS2 in SARS-CoV-2 infection, these findings suggest that the chromium (III)-based compound at doses of 300–600 μg/mL effectively suppresses the protein expression of TMPRSS2 and ACE2, thus preventing SARS-CoV-2 infection in the cellular model.

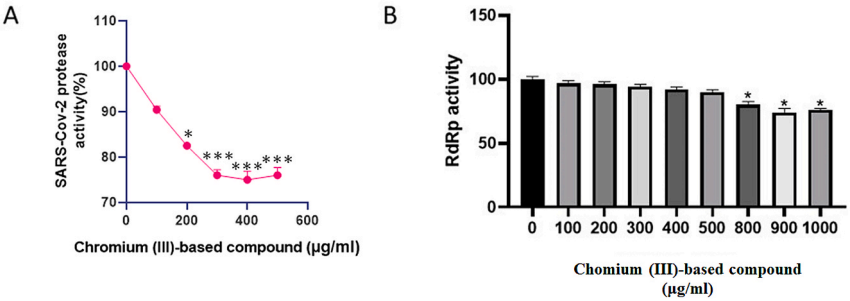

Fig. 5. Dose-dependent decrease in the activity of 3CL protease and RdRp by the chromium (III)-based compound. (A) Effects of different doses of the chromium (III)-based compound on 3CL protease activity. The results show that the compound at concentrations ranging from 100 to 400 μg/mL reduced 3CL protease activity. (B) The greatest decrease in RdRp activity was observed at concentrations of 800–1000 μg/mL of the chromium (III)-based compound. *$p < 0.05$.

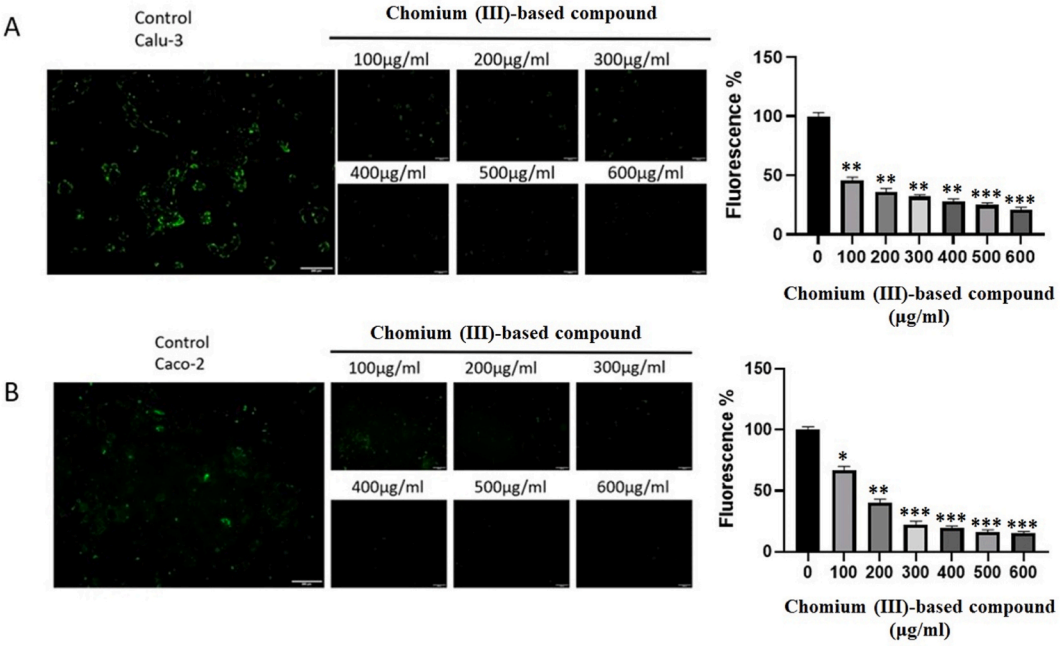

Fig. 6. Effect of the chromium (III)-based compound on SARS-CoV-2 S-pseudotyped lentivirus penetration in ACE-rich Calu-3 and Caco-2 cells. (A) Calu-3 and (B) Caco-2 cells infected with Alpha (B.1.1.7) SARS-CoV-2 S-pseudotyped lentivirus displayed green fluorescence when treated with 100, 200, 300, 400, 500, or 600 μg/mL of the chromium (III)-based compound compared to the control. *$p < 0.05$; **$p < 0.01$; ***$p < 0.001$.

3.3. Reduction of 3CL protease and RdRp activities by the chromium (III)-based compound

The 3CL protease and RdRp play crucial roles in viral maturation and replication. In order to assess the inhibitory effects of the chromium (III)-based compound on the activity of 3CL protease and RdRp, we employed the SensoLyte® 520 SARS-CoV-2 3CL protease activity assay kit and viral RdRp assay kits. The results from the SARS-CoV-2 3CL protease activity assay demonstrated a pronounced dose-dependent inhibitory effect of the chromium (III)-based compound on 3CL protease activity (Fig. 5A). Similarly, the RdRp activity assay revealed that the chromium (III)-based compound inhibited SARS-CoV-2 replication at higher doses (800–1000 μg/mL, Fig. 5B). However, lower doses of the chromium (III)-based compounds exhibited a less significant impact on RdRp activity. Collectively, the chromium (III)-based compounds effectively suppressed the activities of 3CL protease and RdRp, thereby inhibiting viral maturation and replication.

3.4. Chromium (III)-based compound inhibits infection of SARS-CoV-2 spike protein-pseudotyped variant lentiviruses in ACE2-rich bronchial cells (Calu-3) and colorectal cells (Caco-2)

Both Calu-3 and Caco-2 cells infected with alpha (B.1.1.7) SARS-CoV-2 spike protein-pseudotyped lentivirus displayed strong green fluorescence, indicating successful viral adhesion and entry of viral RNA. However, the green fluorescence intensity was reduced in both Calu-3 and Caco-2 cells following pretreatment with 100–600 μg of a chromium (III)-based compound. This compound effectively inhibited the entry of alpha (B.1.1.7) SARS-CoV-2 spike protein-pseudotyped viruses into the cells (Fig. 6). Similarly, ACE2-rich cells infected with Beta (N501Y·V2), Gamma (P1), and Delta (B.1.617.2) SARS-CoV-2 spike protein-pseudotyped lentivirus exhibited significant fluorescence, indicating successful viral adhesion and entry of viral RNA. However, pretreatment with 100–600 μg of the chromium (III)-based compound led to a reduction in fluorescence intensity (Fig. 7). These results demonstrate that the Alpha, Beta, Gamma, and Delta variants of SARS-CoV-2 pseudotyped viruses showed strong fluorescence in Calu-3 and Caco-2 cells, but the chromium (III)-based compound significantly decreased the fluorescence intensity, indicating the inhibition of viral entry into lung and colorectal cells. Thus, the chromium (III)-based compound exhibited inhibitory effects against SARS-CoV-2 variants with high

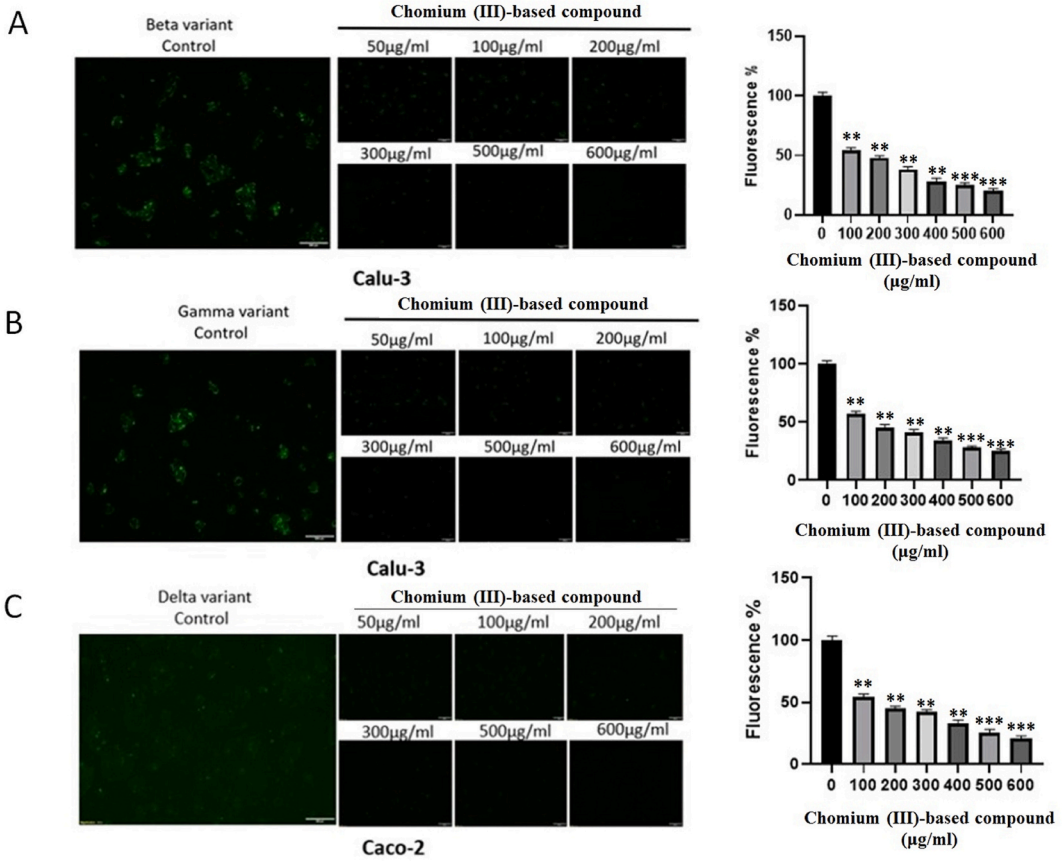

Fig. 7. Effect of the chromium (III)-based compound on Beta, Gamma, and Delta variants of SARS-CoV-2 S-pseudotyped lentivirus with high transmission rates. Caco-2 and Calu-3 cells infected with SARS-CoV-2 S-pseudotyped lentivirus variants were treated with 50, 100, 200, 300, 500, or 600 μg/mL of the chromium (III)-based compound compared to the control. (A) Beta variant, (B) Gamma variant, and (C) Delta variant. $^{**}p < 0.01$; $^{***}p < 0.001$.

transmission and infection rates, including the alpha, beta, gamma, and delta variants.

3.5. Chromium (III)-based compound effectively reduces wild-type SARS-CoV-2 accumulation in the thorax and abdomen of SKH1 mice

We investigated the efficacy of a chromium (III)-based compound *in vivo* using SKH1 mice infected with a wild-type SARS-CoV-2 spike protein-pseudotyped lentivirus. The mice were pretreated with the chromium (III)-based compound three days prior to lentivirus infusion, and viral accumulation was assessed on day 7 using IVIS imaging (Fig. 8A). Challenge with the wild-type SARS-CoV-2 spike protein-pseudotyped lentivirus on day 4 led to SARS-CoV-2 infection in the SKH1 mice. IVIS imaging on day 7 revealed the viral load in the thorax and abdomen of the control mice. Pretreatment with the chromium (III)-based compound at doses of 10 and 100 mg/mouse/day demonstrated a significant dose-dependent inhibition of the viral load of wild-type SARS-CoV-2 in both the thorax and abdomen of the mice (Fig. 8B). Compared to the control group, the reduction in viral accumulation was lower in the 10 mg/mouse/day group, with an 80% reduction in the nasopharynx and a 56% reduction in the gut. In contrast, the 100 mg/mouse/day group exhibited a greater reduction in viral accumulation, with an 85% reduction in the nasopharynx and a 90% reduction in the gut compared to the control group. Therefore, oral administration of the chromium (III)-based compound may effectively reduce the systemic accumulation of SARS-CoV-2.

3.6. Chromium (III)-based compound effectively inhibits viral infection by multiple variants of SARS-CoV-2 spike protein-pseudotyped lentivirus in abdomen and thorax of SKH1 mice

The administration of the chromium (III)-based compound effectively reduced viral accumulation of various variants of SARS-CoV-2 spike protein-pseudotyped lentivirus. Oral treatment with the compound at doses of 10 mg/mouse/day and 100 mg/mouse/day resulted in reduced infection by SARS-CoV-2 spike protein-delta-pseudotyped lentivirus (Delta variant, Fig. 9A). Compared to the control group, the 10 mg/mouse/day group exhibited a 50% reduction in viral accumulation in the nasopharynx and a 30% reduction in the gut. In contrast, the 100 mg/mouse/day group demonstrated a more significant reduction, with an 86% reduction in the

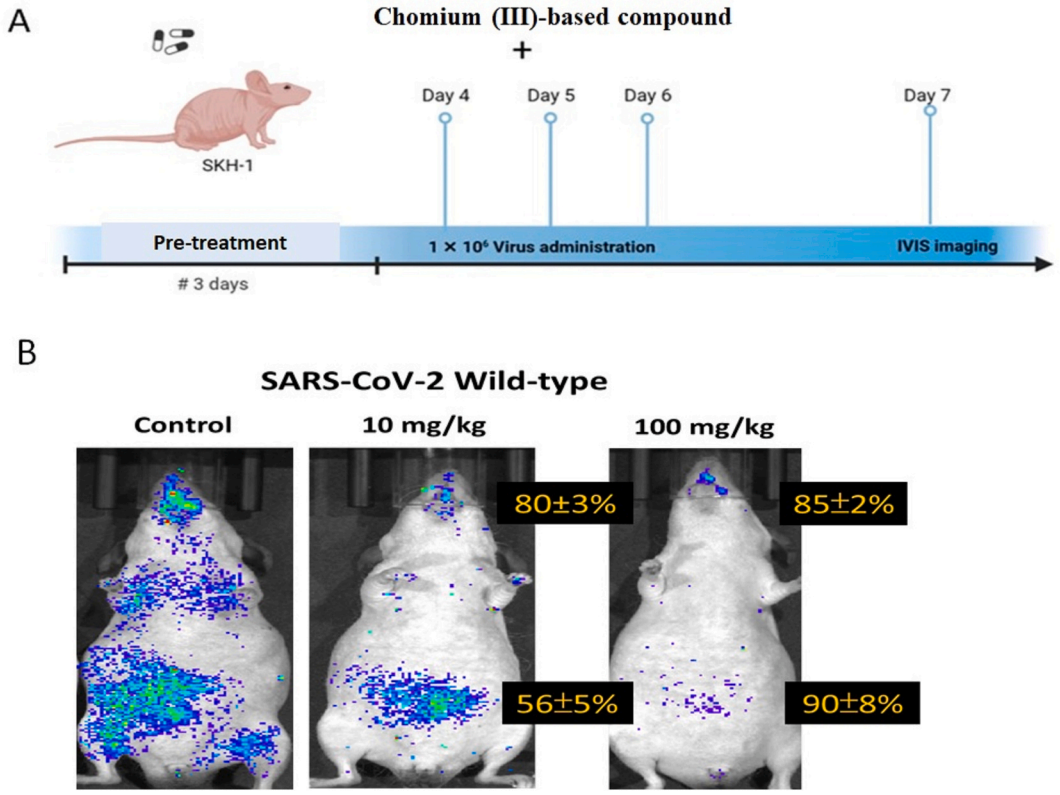

Fig. 8. Effect of the chromium (III)-based compound in reducing viral load in the thorax and abdomen. (A) Schematic diagram of the *in vivo* infection protocol: 6–8-week-old female SKH1 mice were pretreated with the chromium (III)-based compound (10 mg and 100 mg) for three days. Then, for the next three days, mice were infected with SARS-CoV-2 pseudolentivirus intranasally while continuing chromium (III)-based compound administration. On the seventh day, viral load accumulation was visualised using IVIS. (B) Infection with SARS-CoV-2 wild type commenced on Day 3 and continued for three consecutive days. A dose-dependent comparison was made between the control group and mice treated with 10 and 100 mg/day of the chromium (III)-based compound.

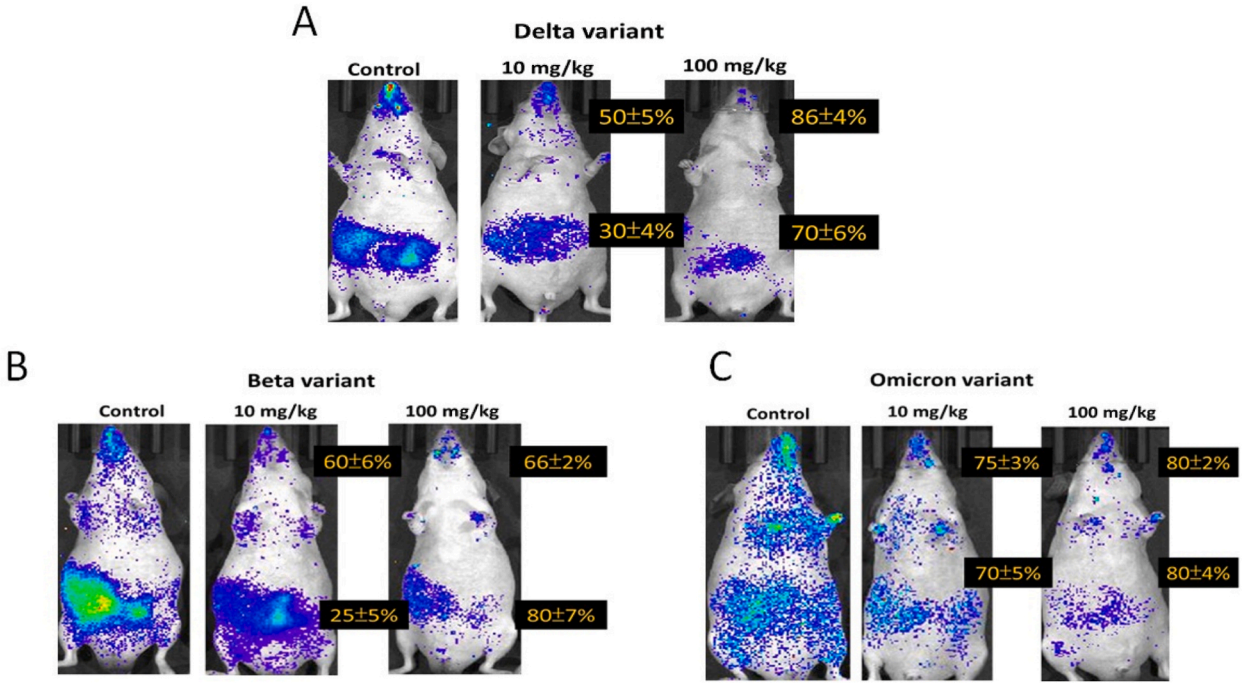

Fig. 9. Effect of chromium (III)-based compound administration on the accumulation of SARS-CoV-2 variants in SKH1 mice. SKH1 mice were pretreated with chromium (III)-based compounds (10 mg and 100 mg) for three days. Infection with different SARS-CoV-2 variants commenced on day 3 and continued for three consecutive days. On the seventh day, viral load accumulation was visualised using IVIS. A dose-dependent comparison was made between the control group and mice treated with 10 mg/day and 100 mg/day of the chromium (III)-based compounds. (A) Delta variant, (B) Beta variant, and (C) Omicron variant.

nasopharynx and a 70% reduction in the gut. Similarly, for the SARS-CoV-2 spike protein-beta-pseudotyped lentivirus (Beta variant, Fig. 9B), the 10 mg/mouse/day group displayed a lesser reduction in viral accumulation, with a 60% reduction in the nasopharynx and a 25% reduction in the gut compared to the control group. However, the 100 mg/mouse/day group exhibited a greater reduction, with a 66% reduction in the nasopharynx and an 80% reduction in the gut compared to the control group. Additionally, in the case of the SARS-CoV-2 spike protein-Omicron-pseudotyped lentivirus (Omicron variant, Fig. 9C), the 10 mg/mouse/day group exhibited a lower reduction in viral accumulation, with a 75% reduction in the nasopharynx and a 70% reduction in the gut compared to the control group. Conversely, the 100 mg/mouse/day group demonstrated a greater reduction, with an 80% reduction in the nasopharynx and an 80% reduction in the gut compared to the control group. These findings indicate that the chromium (III)-based compound can prevent and reduce infection by multiple variants of SARS-CoV-2 *in vivo*.

4. Discussion

Due to the ongoing COVID-19 pandemic and the emergence of new SARS-CoV-2 variants, the development of new medications to prevent SARS-CoV-2 infection and reduce the severity of COVID-19 remains crucial. In this article, we discuss strategies for developing anti-SARS-CoV-2 compounds and provide some examples. Scientists are currently focusing on targeting the SARS-CoV-2 life cycle to develop inhibitors of viral infection. For instance, both ACE2 and TMPRSS2 play essential roles in the attachment of SARS-CoV-2 and facilitate fusion with host cells. Previous research has shown that cepharantine and hesperidin can inhibit the interaction between ACE2 and the SARS-CoV-2 spike protein [20,26,27]. The infection of cells by SARS-CoV-2 through TMPRSS2 can be hindered by aprotinin, camostat, or nafamostat [27]. SARS-CoV-2 enters host cells via endosomes, and pH and cathepsins are key factors determining viral entry through the endosomal pathway. Teicoplanin, a cathepsin inhibitor, directly prevents viral genome entry into the cytoplasm [28]. Additionally, compounds such as azithromycin, chloroquine, and hydroxychloroquine indirectly inhibit viral genome entry by altering pH levels and suppressing cathepsin activity [26,27]. However, the efficacy of chloroquine and hydroxychloroquine against SARS-CoV-2 has been observed primarily *in vitro*, as clinical trials have demonstrated no significant effects on the clinical outcomes of COVID-19 patients, raising concerns about adverse events such as damage to the retina, liver, skeletal, and cardiac muscle cells due to their affinity for lysosomes. The FDA initially granted emergency use authorisation for hydroxychloroquine against COVID-19 in March 2020, but this authorisation was revoked on June 15th, 2020 [29,30]. Other potential targets for COVID-19 treatment are 3C-like protease and RdRp, two enzymes involved in viral replication after the viral genome is released into the cytoplasm.

Baicalin and baicalein, components of *Scutellaria baicalensis*, can inhibit 3C-like protease activity. Paxlovid, which contains

nirmatrelvir and ritonavir, also inhibits 3C-like protease activity [31]. Favipiravir, remdesivir, and molnupiravir inhibit viral RNA replication by targeting RdRp [14,26,32]. Paxlovid, remdesivir, and molnupiravir have all been used in clinical settings to treat COVID-19 patients.

In this study, we introduce a novel chromium (III)-based compound named hexaacetotetraaquadihydroxochromium(III)diiron(III) nitrate $[CrFe_2(CH_3CO_2)_6(H_2O)_4(OH)_2]^{+}NO_3^{-}$ (Fig. 1) and demonstrate its antiviral activity. The molecular weight of the compound is 686.11, with the following elemental composition: Cr, 7.36%; Fe, 19.31%; N, 2.21%; C, 21.73%; H, 3.86%; and O, 44.21%. Treatment with 100 μg/mL of this compound significantly reduced more than 50% of the interactions between the SARS-CoV-2 spike protein and ACE2 (Fig. 2). Moreover, the chromium (III)-based compounds exhibited no significant cytotoxicity in terms of inhibiting cell growth (Fig. 3). However, treatment with this compound resulted in a reduction in the expression of ACE2 and TMPRSS2 in cells (Fig. 4). Higher doses of the chromium (III)-based compounds further reduced the activities of 3C-like protease and RdRp (Fig. 5). These findings provide evidence that chromium (III)-based compounds can target multiple stages of the viral life cycle. In comparison to compounds or drugs that specifically inhibit the ACE2 and TMPRSS2 pathways of SARS-CoV-2 entry, the chromium (III)-based compound not only prevents SARS-CoV-2 infection but also restricts viral replication within host cells, thus preventing severe infection in the body. Therefore, the use of chromium (III)-based compounds represents a multifaceted approach to prevent SARS-CoV-2 infections.

To investigate the efficacy of the chromium (III)-based compound in blocking the entry of pseudovirus variants into ACE2-rich cells, we utilised fluorescent SARS-CoV-2 spike protein-pseudotyped lentiviral particles (Figs. 6 and 7). Treatment with the chromium (III)-based compound resulted in a reduced entry of pseudovirus variants. *In vivo* studies also demonstrated reduced levels of pseudovirus accumulation in the abdomen and thorax of treated mice (Figs. 8 and 9). Importantly, the antiviral efficiency was higher in the high dose group compared to the low dose group. These findings suggest that chromium (III)-based compounds warrant further investigation as potential agents for the prevention and treatment of SARS-CoV-2 infections.

While this novel small Cr (III)-based compound shows promise in the treatment of COVID-19, there are some limitations to this study. The functional activities of the 3CL protease and RdRp were determined using commercial kits in the viral enzyme assay, and data from cell models were not included. It should be noted that the ACE2-rich Calu-3 and Caco-2 cell lines used in the study are cancer cells and may respond slightly differently to chromium (III)-based compounds compared to normal cells. Additionally, the study only included a few common SARS-CoV-2 variants. Given the rapid mutation rate of SARS-CoV-2, future investigations should include a

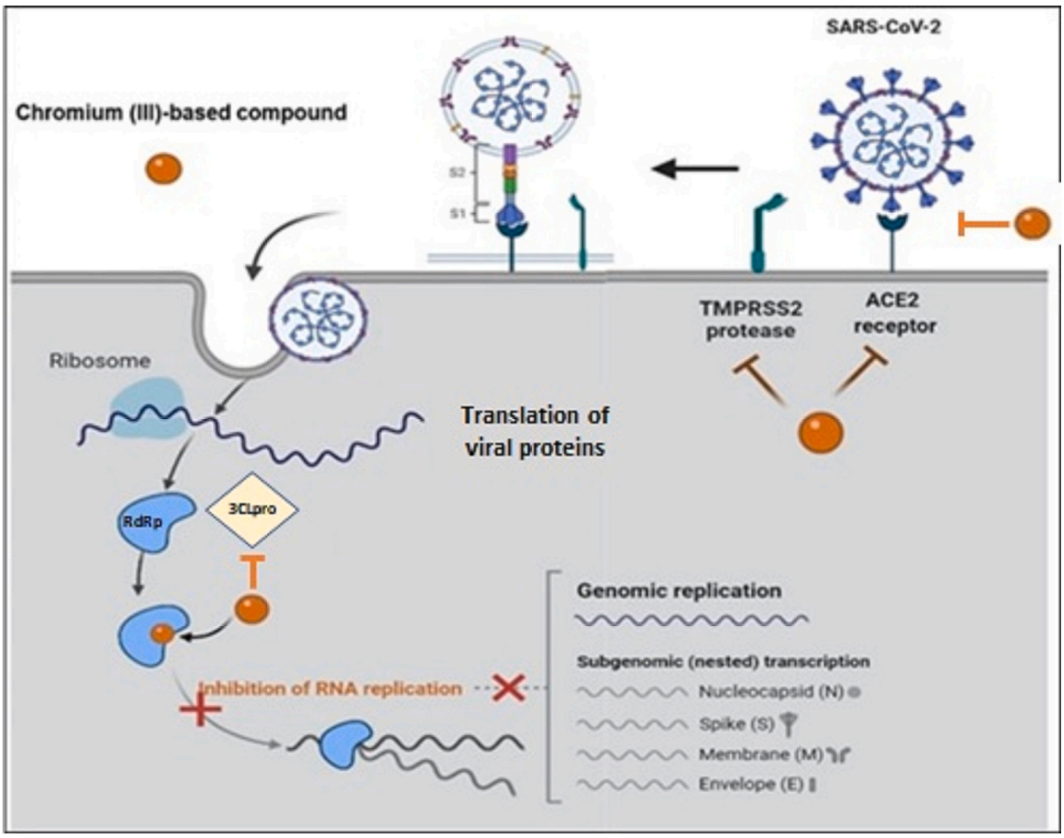

Fig. 10. Proposed model of potential targets for the chromium (III)-based compound in the SARS-CoV-2 life cycle. Selected mechanisms of SARS-CoV-2 pathogenesis targeted by the chromium (III)-based compound: Binding of the viral spike protein of SARS-CoV-2 to ACE2 and priming of the spike protein of SARS-CoV-2 by TMPRSS2. Suppression of 3CL protease and replication activity of SARS-CoV-2.

broader range of variants to assess the therapeutic effects of chromium (III)-based compounds. Lastly, due to national regulations and limited equipment availability, only SARS-CoV-2 spike protein-pseudotyped lentivirus, and not the actual SARS-CoV-2 virus, was used for *in vitro* and *in vivo* experiments. However, clinical trials are planned to further evaluate the potential of chromium (III)-based compounds. Despite these limitations, we believe that small Cr (III)-based compounds have the potential to be effective in the prevention and treatment of COVID-19.

5. Conclusion

Due to the SARS-CoV-2 pandemic, new strategies are necessary to prevent and treat viral infections. In this study, we introduce a novel compound based on chromium (III) that shows promise in preventing SARS-CoV-2 infection. This compound directly inhibits the interaction between the spike protein of SARS-CoV-2 and ACE2. Moreover, it leads to reduced expression levels of ACE2 and TMPRSS2 in cells. The compound also demonstrates inhibitory effects on the functional activities of 3CL protease and RdRp, as observed in the viral enzyme assay (Fig. 10). Furthermore, in an *in vitro* model, it significantly reduces the entry of pseudoviral variants into cells. Consistently, in an *in vivo* animal model, treatment with this novel compound leads to reduced viral accumulation in the abdomen and thorax. Overall, this small compound based on chromium (III) demonstrates potential in reducing SARS-CoV-2 infection by targeting various stages of the viral life cycle, and thus merits further investigation as a novel therapy for COVID-19.

Author contribution statement

Yu-Jung Lin: Conceived and designed the experiments; Contributed reagents, materials, analysis tools or data; Wrote the paper. Chih-Yang Huang: Conceived and designed the experiments; Contributed reagents, materials, analysis tools or data. Hema Sri Devi, Navaneethan Sundhar, Bruce Chi-Kang Tsai: Performed the experiments; Analysed and interpreted the data; Wrote the paper. Hsueh-Fa Pien, Shina Fong-Mei Wen, Jenn-Line Sheu: Contributed reagents, materials, analysis tools or data.

Funding statement

This research was supported by TOMA Biotechnology CO., LTD. and Hualien Tzu Chi Hospital, Buddhist Tzu Chi Medical Foundation (IMAR-110-01-14 and (IMAR-109-01-04-03).

Data availability statement

Data will be made available on request.

Ethics statement

All experiments were conducted in accordance with the protocols of the Institutional Animal Care and Ethics Committee (IACUC) of Hualien Tzu Chi Hospital, Hualien, Taiwan (approval number 109–50).

Consent for publication

All authors have agreed to the publication of this manuscript.

Availability of data and material

The raw data used and/or analysed in the current study are available from the corresponding author upon reasonable request.

Declaration of competing interest

The authors declare that they have no known competing financial interests or personal relationships that could have appeared to influence the work reported in this paper.

Acknowledgements

This research was supported by Miss Feng-Mei Wen and the Chairman of TOMA Biotechnology CO., LTD. We would like to express our gratitude to our colleagues at TOMA Biotechnology Co., Ltd. (Taipei, Taiwan) for their valuable insights and expertise that greatly contributed to this research. We also acknowledge the funding provided by Hualien Tzu Chi Hospital, Buddhist Tzu Chi Medical Foundation (IMAR-110-01-14 and IMAR-109-01-04-03) and Dr. Tzu-Kai Lin provided SKH1 mice for this study.

Appendix A. Supplementary data

Supplementary data to this article can be found online at https://doi.org/10.1016/j.heliyon.2023.e20011.

References

[1] R. Lu, X. Zhao, J. Li, et al., Genomic characterisation and epidemiology of 2019 novel coronavirus: implications for virus origins and receptor binding, Lancet 395 (10224) (2020) 565–574, https://doi.org/10.1016/S0140-6736(20)30251-8.

[2] N. Zhu, D. Zhang, W. Wang, et al., A novel coronavirus from patients with pneumonia in China, 2019, N. Engl. J. Med. 382 (8) (2020) 727–733, https://doi.org/10.1056/NEJMoa2001017.

[3] C.C. Lai, T.P. Shih, W.C. Ko, H.J. Tang, P.R. Hsueh, Severe acute respiratory syndrome coronavirus 2 (SARS-CoV-2) and coronavirus disease-2019 (COVID-19): the epidemic and the challenges, Int. J. Antimicrob. Agents 55 (3) (2020), 105924, https://doi.org/10.1016/j.ijantimicag.2020.105924.

[4] P. Zhou, X. Yang, X.-G. Wang, et al., A pneumonia outbreak associated with a new coronavirus of probable bat origin, Nature 579 (7798) (2020) 270–273, https://doi.org/10.1038/s41586-020-2012-7.

[5] C.B. Creech, S.C. Walker, R.J. Samuels, SARS-CoV-2 vaccines, JAMA 325 (13) (2021) 1318–1320, https://doi.org/10.1001/jama.2021.3199.

[6] C. Del Rio, S.B. Omer, P.N. Malani, Winter of Omicron—the evolving COVID-19 pandemic, JAMA 327 (4) (2022) 319–320, https://doi.org/10.1001/jama.2021.24315.

[7] M. Mohiuddin, K. Kasahara, Investigating the Aggressiveness of the COVID-19 Omicron Variant and Suggestions for Possible Treatment Options, Elsevier, 2021, 106716.

[8] R. Yadav, J.K. Chaudhary, N. Jain, P.K. Chaudhary, S. Khanra, P. Dhamija, A. Sharma, A. Kumar, S. Handu, Role of structural and non-structural proteins and therapeutic targets of SARS-CoV-2 for COVID-19, Cells 10 (4) (2021) 821, https://doi.org/10.3390/cells10040821.

[9] M. Hoffmann, H. Kleine-Weber, S. Schroeder, et al., SARS-CoV-2 cell entry depends on ACE2 and TMPRSS2 and is blocked by a clinically proven protease inhibitor, Cell 181 (2) (2020) 271–280.e8, https://doi.org/10.1016/j.cell.2020.02.052.

[10] D. Schutz, Y.B. Ruiz-Blanco, J. Munch, F. Kirchhoff, E. Sanchez-Garcia, J.A. Muller, Peptide and peptide-based inhibitors of SARS-CoV-2 entry, Adv. Drug Deliv, Rev. E. 167 (2020) 47–65, https://doi.org/10.1016/j.addr.2020.11.007.

[11] R.K. Guy, R.S. DiPaola, F. Romanelli, R.E. Dutch, Rapid repurposing of drugs for COVID-19, Science 368 (6493) (2020) 829–830, https://doi.org/10.1126/science.abb9332.

[12] W. Zhu, C.Z. Chen, K. Gorshkov, M. Xu, D.C. Lo, W. Zheng, RNA-dependent RNA polymerase as a target for COVID-19 drug discovery, SLAS Discov 25 (10) (2020) 1141–1151, https://doi.org/10.1177/2472555220942123.

[13] W.S.T. Consortium, Remdesivir and three other drugs for hospitalised patients with COVID-19: final results of the WHO Solidarity randomised trial and updated meta-analyses, Lancet 399 (10339) (2022) 1941–1953, https://doi.org/10.1016/S0140-6736(22)00519-0.

[14] A. Jayk Bernal, M.M. Gomes da Silva, D.B. Musungaie, et al., Molnupiravir for oral treatment of Covid-19 in nonhospitalized patients, N. Engl. J. Med. 386 (6) (2022) 509–520, https://doi.org/10.1056/NEJMoa2116044.

[15] J. Hammond, H. Leister-Tebbe, A. Gardner, et al., Oral nirmatrelvir for high-risk, nonhospitalized adults with Covid-19, N. Engl. J. Med. 386 (15) (2022) 1397–1408, https://doi.org/10.1056/NEJMoa2118542.

[16] B. Cao, Y. Wang, D. Wen, et al., A trial of lopinavir–ritonavir in adults hospitalized with severe Covid-19, N. Engl. J. Med. 382 (19) (2020) 1787–1799, https://doi.org/10.1056/NEJMoa2001282.

[17] A. Parasher, COVID-19: current understanding of its pathophysiology, clinical presentation and treatment, Postgrad. Med. 97 (1147) (2021) 312–320, https://doi.org/10.1136/postgradmedj-2020-138577.

[18] S. Mehandru, M. Merad, Pathological sequelae of long-haul COVID, Nat. Immunol. 23 (2) (2022) 194–202, https://doi.org/10.1038/s41590-021-01104-y.

[19] R.K.-L. Lee, T.-N. Li, S.-Y. Chang, et al., Identification of entry inhibitors against delta and omicron variants of SARS-CoV-2, Int. J. Mol. Sci. 23 (7) (2022) 4050, https://doi.org/10.3390/ijms23074050.

[20] F.-J. Cheng, T.-K. Huynh, C.-S. Yang, et al., Hesperidin is a potential inhibitor against SARS-CoV-2 infection, Nutrients 13 (8) (2021) 2800, https://doi.org/10.3390/nu13082800.

[21] S.-P. Liu, M.A. Shibu, F.-J. Tsai, et al., Tetramethylpyrazine reverses high-glucose induced hypoxic effects by negatively regulating HIF-1α induced BNIP3 expression to ameliorate H9c2 cardiomyoblast apoptosis, Nutr. Metab. 17 (2020), https://doi.org/10.1186/s12986-020-0432-x, 12-12.

[22] W.S. Chang, C.W. Tsai, J.S. Yang, Y.M. Hsu, L.C. Shih, H.Y. Chiu, D.T. Bau, F.J. Tsai, Resveratrol inhibited the metastatic behaviors of cisplatin-resistant human oral cancer cells via phosphorylation of ERK/p-38 and suppression of MMP-2/9, J. Food Biochem. 45 (6) (2021), e13666, https://doi.org/10.1111/jfbc.13666.

[23] S.-Y. Lu, W.-Z. Hong, B.C.-K. Tsai, Y.-C. Chang, C.-H. Kuo, T.G. Mhone, R.-J. Chen, W.-W. Kuo, C.-Y. Huang, Angiotensin II prompts heart cell apoptosis via AT1 receptor-augmented phosphatase and tensin homolog and miR-320-3p functions to enhance suppression of the IGF1R-PI3K-AKT survival pathway, J. Hypertens. 40 (12) (2022) 2502–2512, https://doi.org/10.1097/HJH.0000000000003285.

[24] C.H. Lai, D. Van Thao, B.C.-K. Tsai, et al., Insulin-like growth factor II receptor alpha overexpression in heart aggravates hyperglycemia-induced cardiac inflammation and myocardial necrosis, Environ. Toxicol. 38 (3) (2023) 676–684, https://doi.org/10.1002/tox.23717.

[25] S.-H. Chang, P.-Y. Pai, C.-H. Hsu, et al., Estimating the impact of drug addiction causes heart damage, Drug Chem. Toxicol. (2022) 1–7, https://doi.org/10.1080/01480545.2022.2122984.

[26] R. Xiang, Z. Yu, Y. Wang, et al., Recent advances in developing small-molecule inhibitors against SARS-CoV-2, Acta Pharm. Sin. B 12 (4) (2022) 1591–1623, https://doi.org/10.1016/j.apsb.2021.06.016.

[27] L. Chitsike, P. Duerksen-Hughes, Keep out! SARS-CoV-2 entry inhibitors: their role and utility as COVID-19 therapeutics, Virol. J. 18 (1) (2021) 1–17, https://doi.org/10.1186/s12985-021-01624-x.

[28] F. Yu, T. Pan, F. Huang, et al., Glycopeptide antibiotic teicoplanin inhibits cell entry of SARS-CoV-2 by suppressing the proteolytic activity of cathepsin L, Front. Microbiol. 13 (2022), 884034, https://doi.org/10.3389/fmicb.2022.884034.

[29] O. Indari, S. Jakhmola, E. Manivannan, H.C. Jha, An update on antiviral therapy against SARS-CoV-2: how far have we come? Front. Pharmacol. 12 (2021), 632677 https://doi.org/10.3389/fphar.2021.632677.

[30] C. Biguetti, M.T. Marrelli, M. Brotto, Primum non nocere–Are chloroquine and hydroxychloroquine safe prophylactic/treatment options for SARS-CoV-2 (covid-19)? Rev. Saude Publica 54 (68) (2020) 1–5, https://doi.org/10.11606/s1518-8787.2020054002631.

[31] M. Marzi, M.K. Vakil, M. Bahmanyar, E. Zarenezhad, Paxlovid: mechanism of action, synthesis, and in silico study, BioMed Res. Int. 2022 (2022), 7341493, https://doi.org/10.1155/2022/7341493.

[32] U. Agrawal, R. Raju, Z.F. Udwadia, Favipiravir: a new and emerging antiviral option in COVID-19, Med. J. Armed Forces India 76 (4) (2020) 370–376, https://doi.org/10.1016/j.mjafi.2020.08.004.